Defense Threat Reduction Agency
8725 John J. Kingman Road, MS-6201
Fort Belvoir, VA 22060-6201

DTRA-TR-17-019

TECHNICAL REPORT

Utilization of ICU Data to Improve 30 and 60-Day Mortality Models

January 2017

HDTRA1-14-D-0003; 0005

Prepared by:

Applied Research Associates, Inc.
801 N. Quincy Street
Suite 700
Arlington, VA 22203

REPORT DOCUMENTATION PAGE

Form Approved
OMB No. 0704-0188

PLEASE DO NOT RETURN YOUR FORM TO THE ABOVE ADDRESS.

1. REPORT DATE *(DD-MM-YYYY)*	2. REPORT TYPE	3. DATES COVERED *(From - To)*
06-01-2017	Technical Report	

4. TITLE AND SUBTITLE

Utilization of ICU Data to Improve 30 and 60-Day Mortality Models

5a. CONTRACT NUMBER

HDTRA1-14-D-0003/0005

5b. GRANT NUMBER

5c. PROGRAM ELEMENT NUMBER

6. AUTHOR(S)

Bellman, Jacob
Pirone, Jason
Crary, Dave
Beaulieu, Stephen

5d. PROJECT NUMBER

5e. TASK NUMBER

5f. WORK UNIT NUMBER

7. PERFORMING ORGANIZATION NAME(S) AND ADDRESS(ES)

Applied Research Associates, Inc.
801 N. Quincy Street, Suite 700
Arlington, VA 22203

8. PERFORMING ORGANIZATION REPORT NUMBER

9. SPONSORING/MONITORING AGENCY NAME(S) AND ADDRESS(ES)

Nuclear Technologies Department, Attn: Dr. Blake
Defense Threat Reduction Agency
8725 John J. Kingman Road, Mail Stop 6201
Fort Belvoir, VA 22060-6201

10. SPONSOR/MONITOR'S ACRONYM(S)

DTRA J9NTSN

11. SPONSOR/MONITOR'S REPORT NUMBER(S)

DTRA-TR-17-019

12. DISTRIBUTION/AVAILABILITY STATEMENT

DISTRIBUTION A. Approved for public release: distribution is unlimited.

13. SUPPLEMENTARY NOTES

14. ABSTRACT

This report presents the use of available ICU data to extend the capabilities of 30 and 60-day mortality models in the Health Effects from Nuclear and Radiological Environments (HENRE) software. These models relate levels of molecular and cellular biomarkers currently modeled in HENRE to mortality using data from the medical literature. A small intestine injury model predicts the probability of 30-day mortality after radiation and burn combined injuries using the biomarker citrulline, and a platelet reduction model predicts the probability of 60-day mortality after burn. These models have been developed to predict mortality of casualties with access to standard medical care. A review of the literature on the use of the neutrophil to lymphocyte ratio (NLR) as a biomarker of inflammation and mortality is presented. The NLR may be used in future work to further extend the capabilities of the mortality models in HENRE.

15. SUBJECT TERMS

Acute Radiation Syndrome, Mortality, Burn Combined Injury, Lethality, Small Intestine, Ordinary Differential Equations Model, Thrombopoiesis, Granulopoiesis, Lymphopoiesis

16. SECURITY CLASSIFICATION OF:			17. LIMITATION OF ABSTRACT	18. NUMBER OF PAGES	19a. NAME OF RESPONSIBLE PERSON
a. REPORT	b. ABSTRACT	c. THIS PAGE			Dr. Paul Blake, Ph.D.
U	U	U	U	39	19b. TELEPHONE NUMBER *(Include area code)* 703-767-3433

UNIT CONVERSION TABLE

U.S. customary units to and from international units of measurement*

U.S. Customary Units	Multiply by → / ← Divide by†		International Units
Length/Area/Volume			
inch (in)	2.54	$\times 10^{-2}$	meter (m)
foot (ft)	3.048	$\times 10^{-1}$	meter (m)
yard (yd)	9.144	$\times 10^{-1}$	meter (m)
mile (mi, international)	1.609 344	$\times 10^{3}$	meter (m)
mile (nmi, nautical, U.S.)	1.852	$\times 10^{3}$	meter (m)
barn (b)	1	$\times 10^{-28}$	square meter (m^2)
gallon (gal, U.S. liquid)	3.785 412	$\times 10^{-3}$	cubic meter (m^3)
cubic foot (ft^3)	2.831 685	$\times 10^{-2}$	cubic meter (m^3)
Mass/Density			
pound (lb)	4.535 924	$\times 10^{-1}$	kilogram (kg)
atomic mass unit (AMU)	1.660 539	$\times 10^{-27}$	kilogram (kg)
pound-mass per cubic foot ($lb\ ft^{-3}$)	1.601 846	$\times 10^{1}$	kilogram per cubic meter ($kg\ m^{-3}$)
Pound-force (lbf avoirdupois)	4.448 222		Newton (N)
Energy/Work/Power			
electron volt (eV)	1.602 177	$\times 10^{-19}$	joule (J)
erg	1	$\times 10^{-7}$	joule (J)
kiloton (kT) (TNT equivalent)	4.184	$\times 10^{12}$	joule (J)
British thermal unit (Btu) (thermochemical)	1.054 350	$\times 10^{3}$	joule (J)
foot-pound-force (ft lbf)	1.355 818		joule (J)
calorie (cal) (thermochemical)	4.184		joule (J)
Pressure			
atmosphere (atm)	1.013 250	$\times 10^{5}$	pascal (Pa)
pound force per square inch (psi)	6.984 757	$\times 10^{3}$	pascal (Pa)
Temperature			
degree Fahrenheit (°F)	[T(°F) − 32]/1.8		degree Celsius (°C)
degree Fahrenheit (°F)	[T(°F) + 459.67]/1.8		kelvin (K)
Radiation			
activity of radionuclides [curie (Ci)]	3.7	$\times 10^{10}$	per second (s^{-1}‡)
air exposure [roentgen (R)]	2.579 760	$\times 10^{-4}$	coulomb per kilogram ($C\ kg^{-1}$)
absorbed dose (rad)	1	$\times 10^{-2}$	joule per kilogram ($J\ kg^{-1}$§)
equivalent and effective dose (rem)	1	$\times 10^{-2}$	joule per kilogram ($J\ kg^{-1}$**)

*Specific details regarding the implementation of SI units may be viewed at http://www.bipm.org/en/si/.

†Multiply the U.S. customary unit by the factor to get the international unit. Divide the international unit by the factor to get the U.S. customary unit.

‡The special name for the SI unit of the activity of a radionuclide is the becquerel (Bq). ($1\ Bq = 1\ s^{-1}$).

§The special name for the SI unit of absorbed dose is the gray (Gy). ($1\ Gy = 1\ J\ kg^{-1}$).

**The special name for the SI unit of equivalent and effective dose is the sievert (Sv). ($1\ Sv = 1\ J\ kg^{-1}$).

This page intentionally left blank.

Table of Contents

List of Figures

List of Tables

Acknowledgements

The authors of this modeling work acknowledge the technical developments by Dr. Olga Smirnova, who dedicated years of research and modeling efforts to develop the original structure for the cell kinetic models in this research. These models were further developed by members of the ARA team. We would also like to acknowledge the many experimentalists who collected the data that has been crucial for our modeling efforts. Finally, we gratefully acknowledge Dr. Paul Blake of DTRA/J9 for programmatic support. The work was performed under DTRA contract HDTRA1-14-D-0003; 005.

Executive Summary

This report presents mortality models that use biomarkers of the small intestine and thrombopoiesis to predict mortality. These models improve the capabilities of the 30 and 60-day mortality models in HENRE by providing:

- The Small Intestine Mortality Model (SIMM) that represents small intestine epithelial cell kinetics and the amino acid biomarker, citrulline, to predict 30-day mortality. This model predicts the probability of mortality of an individual receiving treatment after being exposed to combined radiation and burn injury.
- The Platelet Attenuation Mortality Model (PAMM) that simulates thrombocyte cell kinetics to predict 60-day mortality. This model predicts the probability of mortality of an individual receiving treatment after being exposed to a burn injury.
- A comprehensive literature review of the neutrophil to lymphocyte ratio (NLR), a biomarker of inflammatory response that describes the potential predictive power of the NLR for various health effects, including mortality. We will discuss the benefits of including an NLR-based mortality model with DTRA and, as appropriate, develop options for a future version of HENRE.

1 Introduction

Applied Research Associates (ARA) has been tasked by the Defense Threat Reduction Agency (DTRA) to support their mission to safeguard the United States against weapons of mass destruction (WMD). ARA is supporting this effort by developing state-of-the-art mathematical models that predict health effects and provide risk assessment of individuals exposed to harmful environments produced by a nuclear weapon. A crucial part of this project is predicting lethality of various combinations of radiation, thermal, and blast insults, which is the focus of this study.

In the event of an improvised nuclear device (IND) detonation, there would be a broad spectrum of casualties with various types of injuries. Probability of mortality for each individual will vary by the amount of exposure to radiation, burn and blast environments and the availability of medical treatment. In order to estimate mortality for this type of scenario, ARA is developing models to estimate 48-hour, 30-day, and 60-day mortality, as well as models to estimate serious injury as a function of time and exposure.

There are limitations for each of the mortality models currently in HENRE. For instance, the 30-day mortality model only accepts burn insults, and assumes the casualty receives no treatment following exposure (Stricklin, 2013a). The 60-day mortality model estimates the probability of mortality following a combined radiation and burn insult (Stricklin, 2013b). When radiation is the only insult provided, this model predicts mortality based on age, gender and available medical treatment (Stricklin, 2016). However, when burn is included, this model does not consider individual demographic differences, and only predicts mortality under the assumption that medical treatment is unavailable. A comprehensive list of lethality models in the latest version of HENRE are reviewed in detail in Oldson et al., 2015 and Stricklin, 2015a.

Figure 1.1 summarizes the current modeling capabilities in HENRE; check marks represent available capabilities and empty squares represent scenarios that will be modeled in the future. The Small Intestine Mortality Model (SIMM) and the Platelet Attenuation Mortality Model (PAMM), both introduced in this report, are shown in the shaded cells.

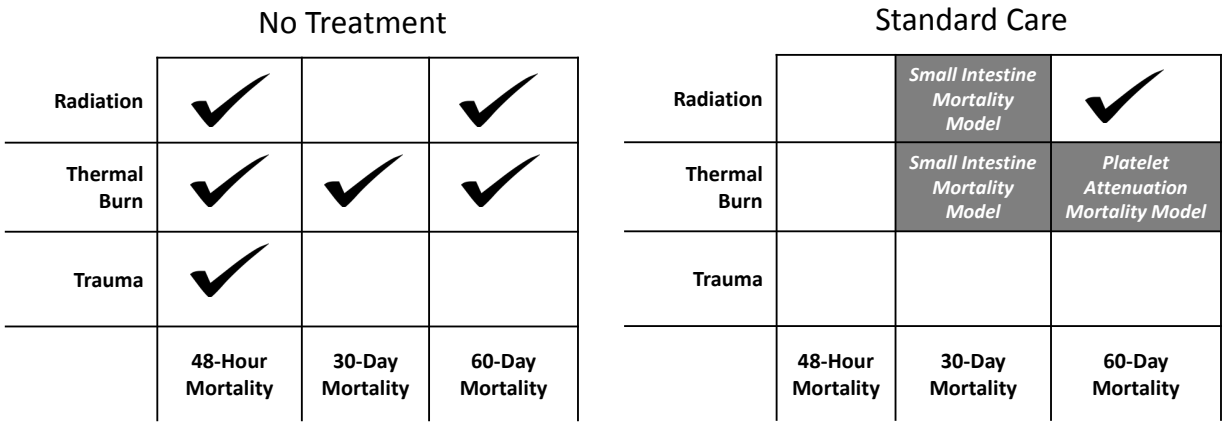

Figure 1.1: Modeling capabilities of HENRE.

2 Purpose

To improve the predictive capabilities of the mortality models in HENRE, we developed models to supplement the 30 and 60-day combined injury mortality models. The new version of the 30-day lethality model (SIMM) couples the small intestine cell kinetics model with a biomarker (citrulline) to predict mortality due to the combined effects of radiation and thermal injury. The new version of the 60-day lethality model (PAMM) uses the thrombocyte cell kinetic model to simulate a biomarker (platelets) to predict 60-day mortality as a function of burn size. The new models (SIMM and PAMM) were developed using intensive care unit (ICU) patient data to represent the standard care scenario shown in Figure 1.1. Figure 2.1 illustrates the overall structure of the two mortality models presented in this report.

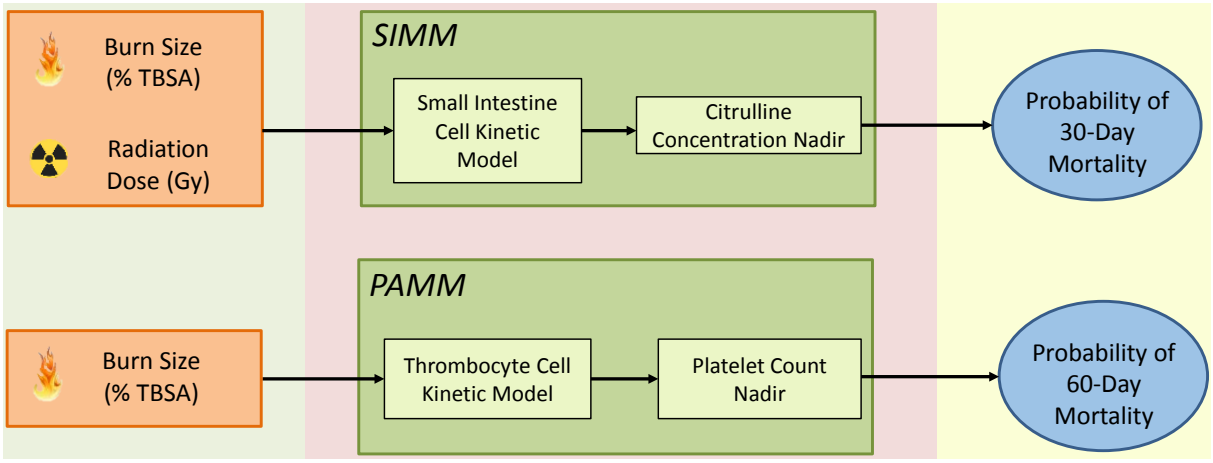

Figure 2.1: Mortality models based on small intestine and thrombocyte cell kinetics.

3 Background

Exposure to a large dose of radiation in a short period of time (high dose rate) causes acute radiation syndrome (ARS). Depending on the radiation dose, an individual may experience the hematopoietic acute radiation syndrome (H-ARS) or the gastrointestinal acute radiation syndrome (GI-ARS) (reviewed in Maciàă I Garau et al., 2011). For acute radiation doses larger than 1 Gray (Gy), damage to stem cell progenitors of hematopoietic cells weakens the immune system and leaves the exposed individual susceptible to infection and bleeding. For radiation doses greater than 6 Gy, damage to small intestine epithelial clonogenic cells leads to a reduction in small intestine epithelial lining. This can cause diarrhea, bacterial translocation, and sepsis as the epithelial lining provides an essential barrier for defense against bacterial invasion into the bloodstream. Due to the recovery time of the different cell systems, these acute radiation sub-syndromes can remain life-threatening for up to 30 days in the case of GI-ARS, and up to 60 days for H-ARS.

Combinations of injuries from radiation, thermal and blast environments cause complex physiological responses that can significantly complicate health risks. Animal studies have quantified the increased effects on the hematopoietic and gastrointestinal systems from combining thermal and blast-related injuries to irradiation (Kiang et al., 2014; Carter et al., 2016; Baker and Valeriote, 1968; Palmer et al., 2011). However, there is minimal human data on combined injuries, making it difficult to model the biological effects of these scenarios. As an alternative approach, we have evaluated the literature for biomarkers that could be used in predicting mortality.

Clinical studies of ICU patients have assessed the prognostic power of various biological measurements as predictive biomarkers of mortality. In Piton et al., 2013, for instance, the amino acid citrulline was determined to be a predictive biomarker of 28-day mortality for critically ill ICU patients. In addition to citrulline, other noteworthy biomarkers of mortality include platelet levels (Vanderschueren et al., 2000; Strauss et al., 2002; Moreau et al., 2007; Marck et al., 2013; Guo et al., 2012; Akca et al., 2002) and the neutrophil-lymphocyte ratio (NLR) (Salciccioli et al., 2015; Akilli et al., 2014; Dilektasli et al., 2016). Biomarkers were evaluated in this study and used to model probability of 30 and 60-day mortality.

4 Methods

4.1 Small Intestine Damage as a Predictor of 30-Day Mortality

4.1.1 Background

The amino acid citrulline is produced in enterocytes in the small intestine. Accordingly, plasma citrulline concentration has been correlated with small intestine epithelial cell mass in humans (Guoyao and Morris, 1998; Curis et al., 2005; Crenn et al., 2000; Jianfeng et al., 2005; Luo et al., 2007; Rhoads et al., 2005), and used as a biomarker of bacterial translocation, sepsis and death (Crenn et al., 2014 Wijnands et al., 2015; Su et al., 2015; Piton et al., 2010; Piton et al., 2013 Piton et al., 2011). Specifically, thresholds of 10 μmol/L (Piton et al., 2010) and 12.2 μmol/L (Piton et al., 2013) have been identified as statistically significant predictors of 28-day mortality for ICU patients, compared to a normal citrulline concentration range of 20-50 μmol/L (Pappas et al., 2002).

Radiation and burn exposure leads to the death of epithelial cells of the small intestine through different pathways; radiation directly kills proliferating crypt cells, and burns primarily kill villus cells. These injury pathways are represented in our approach of modeling cell kinetics (Figure 4.1) to predict time-dependent proliferating crypt cell counts, maturing crypt cell counts, and villus cell counts following radiation and burn (Bellman and Stricklin, 2016). We have recently improved the approach to modeling burn response, as this model has recently undergone improvements which are documented in Appendix A.

Figure 4.2 provides time-dependent villus cell counts (normalized to pre-insult levels) predicted by the small intestine model in the event of a 10 Gy midline tissue (MLT) radiation dose combined with a 20% total body surface area (TBSA) burn. The figure identifies the villus cell nadir, which can be used to quantify epithelial damage in the small intestine. In this case, an approximate 68% reduction in villus cells is predicted from the combined injury approximately 8 days after exposure.

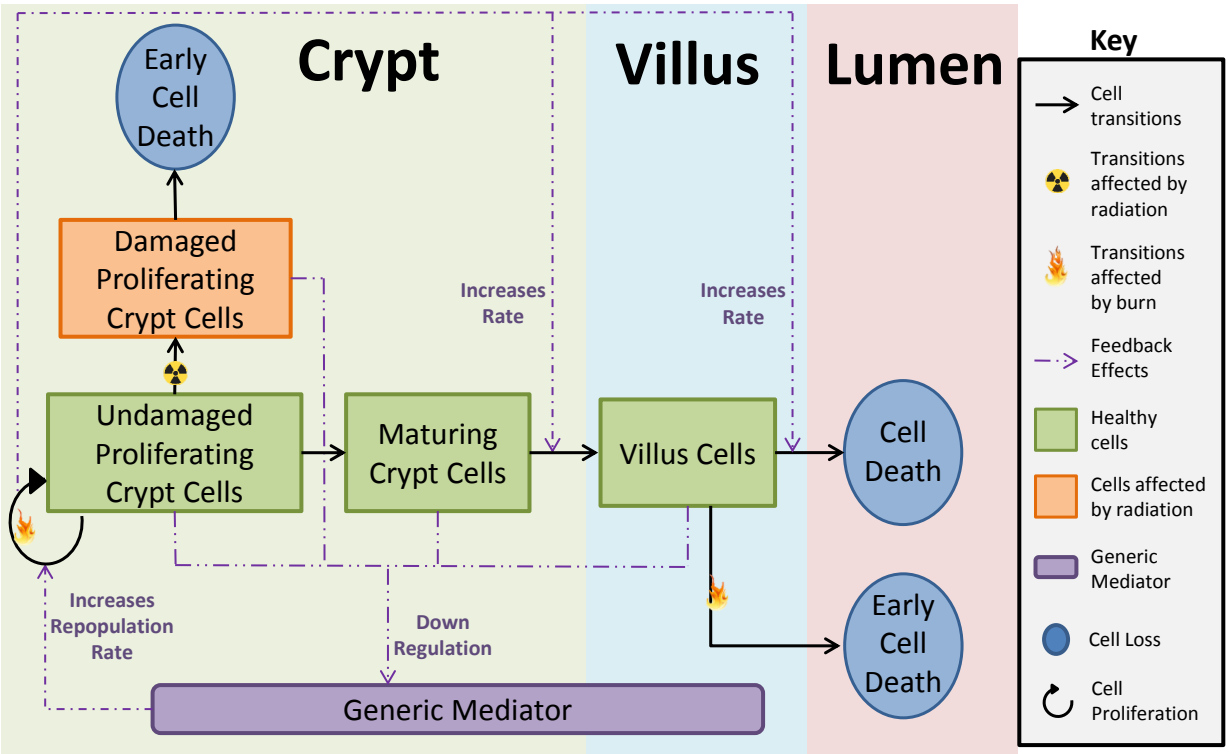

Figure 4.1: Small intestine cell kinetic model.

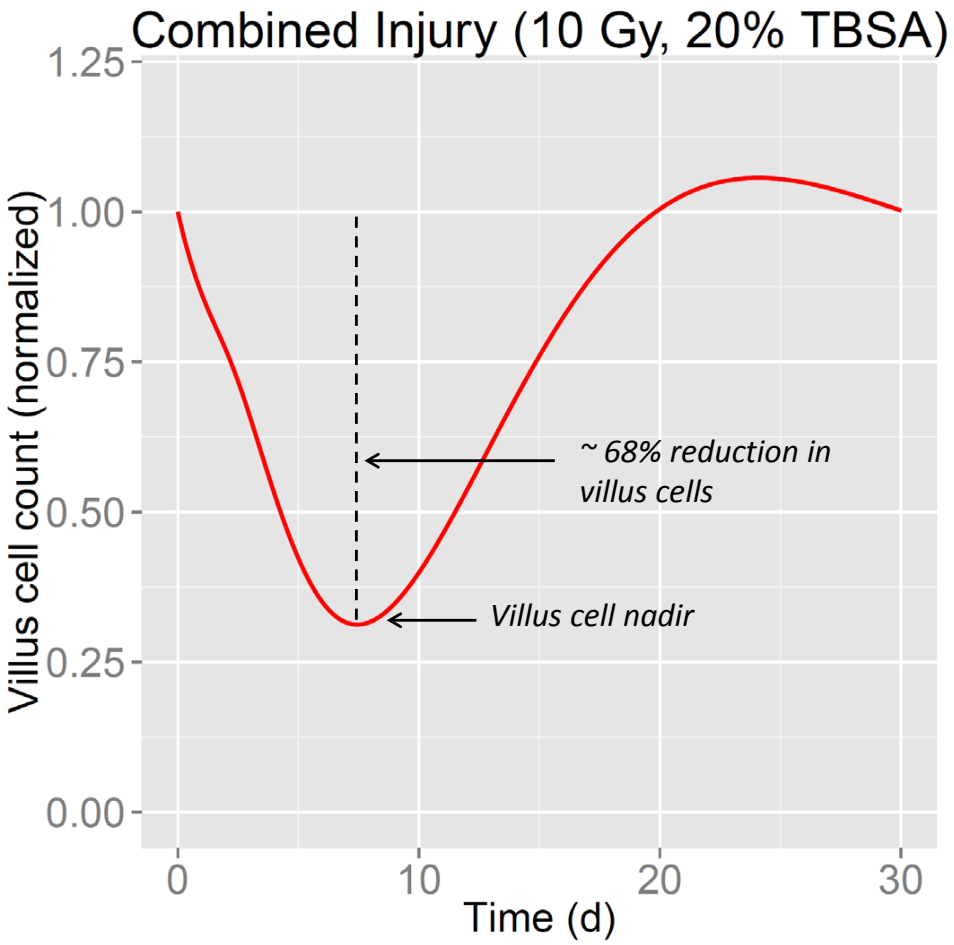

Figure 4.2: Small intestine combined injury example.

4.1.2 30-Day Mortality

In developing the SIMM, we used data from short bowel syndrome (SBS) patients and ICU patients to predict 30-day mortality as a function of villus cell reduction (Bellman, 2016). Briefly, the SBS patient data provide the basis for a rough linear relationship between villus cell populations and citrulline concentration. By establishing a relationship between villus cell populations and citrulline levels, we were able to use ICU patient data to predict the probability of mortality from reduced citrulline levels. This second relationship was complicated by the fact that some patients in the ICU die of conditions that are not necessarily attributable to citrulline levels. To account for this unattributable "baseline" level of mortality, we assumed a constant probability of death for these patients regardless of citrulline levels. We also assumed that the probability of mortality, p_C^d, is dependent on the multiplicative inverse of the citrulline nadir, ci, and follows a log-normal cumulative distribution ($p_C^d(ci) = \int_0^{ci} f_X(t)dt$, where $X \sim \ln\mathcal{N}(\mu, \sigma^2)$). Optimizing this function against the ICU data, we determined optimal location and scale parameters: $\mu = -1.83$, and $\sigma = 0.42$, respectively. The probability of mortality dependent on the citrulline nadir is presented in Figure 4.3.

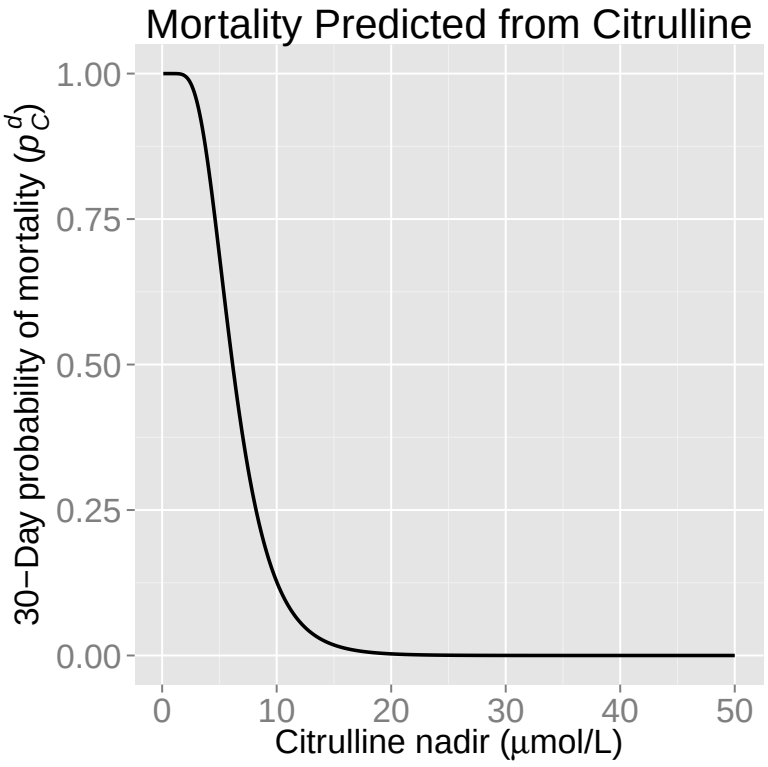

Figure 4.3: 30-Day probability of mortality predicted from citrulline nadir.

4.2 Platelet Loss as a Predictor of 60-Day Mortality

4.2.1 Background

Circulating platelets drop in response to burn insults, which leads to thrombocytopenia, increasing the risk of hemorrhage, hypovolemic shock, sepsis, septic shock and death. Following the drop in platelets, cell count recovery overshoots normal values before a period of prolonged thrombocytosis. This trajectory has consistently been reported in burn patients as well as ICU patients (Marck et al., 2013; Moreau et al., 2007). The minimum platelet count, which generally occurs 3-4 days after ICU admission, is predictive of mortality (Vanderschueren et al., 2000; Akca et al., 2002; Moreau et al., 2007; Guo et al., 2012; Marck et al., 2013).

Our model of thrombopoiesis (Figure 4.4) predicts time-dependent cell counts of mitotic progenitors, megakaryocytes and platelets after combined radiation and burn insults (Wentz et al., 2014a; Wentz et al., 2014b; Wentz et al., 2015) (Figure 4.4). A sample run of the thrombopoiesis model is provided in Figure 4.5, where circulating platelets respond and recover from a 20% TBSA burn. In this case, an approximate 50% reduction in platelets is predicted at the nadir, about four days following the insult.

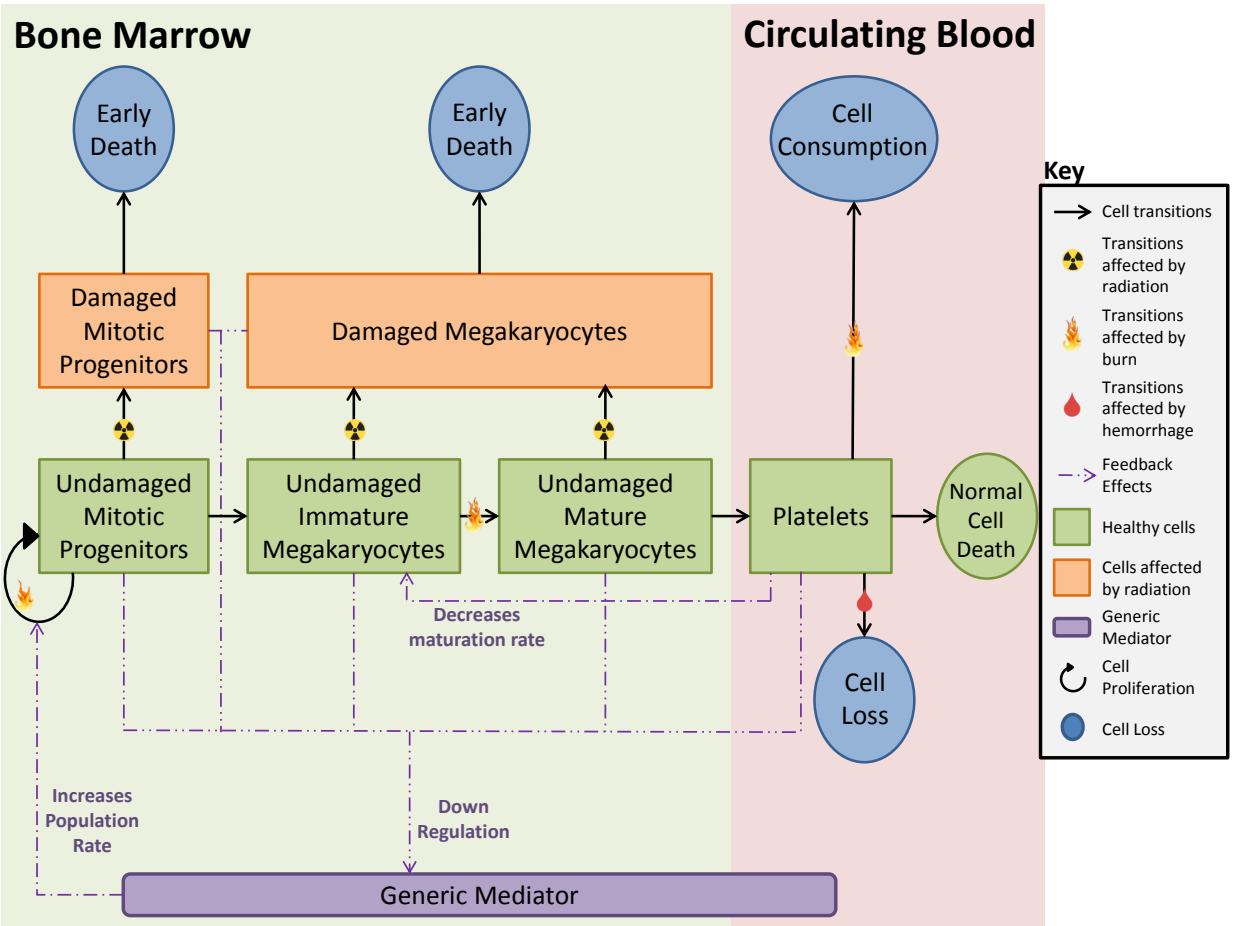

Figure 4.4: Thrombopoiesis cell kinetic model.

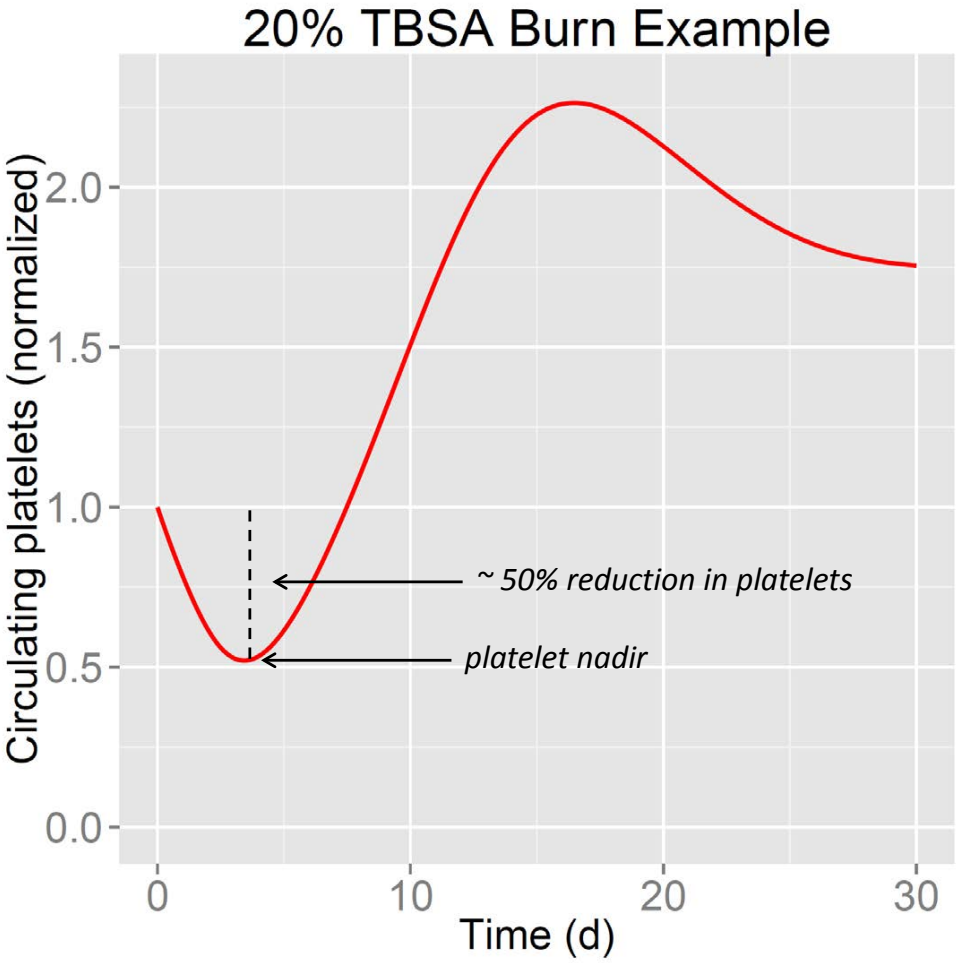

Figure 4.5: Platelet counts of a burn patient.

Radiation injuries yield a different response for circulating platelets, where prolonged thromobcytopenia causes platelets to slowly reach a minimum about 30 days after exposure before returning to normal levels (Bond et al., 1965; Hempelmann et al., 1952; Howland et al., 1961; Mettler, 2001; Stavem et al., 1985). Mortality predicted from a radiation-induced nadir is not consistent with mortality predicted from a burn-induced nadir, so we decided to only focus on burn in this study. In future studies, we will consider alternative biomarkers, such as the duration of thrombocytopenia, that may be more reliable in predicting mortality from combined radiation and burn injuries.

4.2.2 60-Day Mortality

In developing the PAMM, we used data on ICU burn patients to predict the probability of 60-day mortality, p_P^d, given the percent reduction in platelets at the nadir of the platelet trajectory, pr (Crary, 2016). Similar to the SIMM, p_P^d follows a log-normal cumulative distribution ($p_P^d(pr) = \int_0^{pr} f_X(t)dt$, where $X \sim \ln\mathcal{N}(\mu, \sigma^2)$), with the following location and scale parameters: $\mu = 1.83$, and $\sigma = 0.43$. p_P^d is provided in Figure 4.6. Due to data limitations, and the fact that patients can survive after losing over 80% of their platelets

(Guo et al., 2012), this curve does not exceed a probability of mortality of 0.66. We discuss this limitation in Section 6 with respect to the domain of applicability of the model.

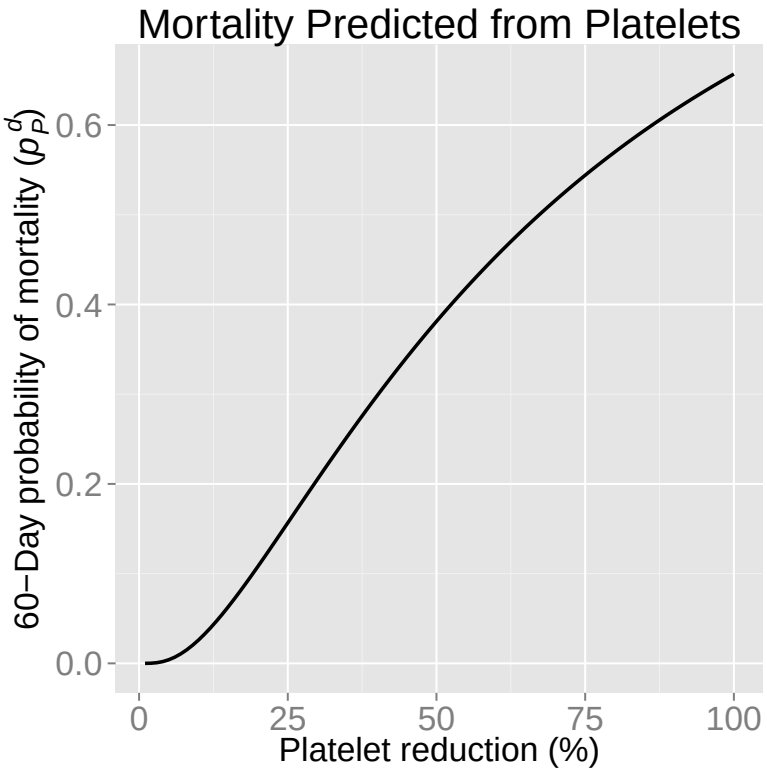

Figure 4.6: 60-Day probability of mortality predicted from platelet nadir.

4.3 Neutrophil to Lymphocyte Ratio

4.3.1 Background

Tissue damage from injury induces a localized inflammatory response involving components of the innate and adaptive immune systems. Soon after injury, the inflammatory response results in changes in the local vasculature that lead to vasodilation, increased vascular permeability, and increased blood flow (Serhan et al., 2010). These changes contribute to the recruitment of leukocytes (white blood cells), plasma proteins, and fluids into the damaged tissue (Ashley et al., 2012). Normally, the perturbations in neutrophil and lymphocyte levels that occur following injury rapidly return to normal. Resolution of inflammation occurs by leucocyte removal by apoptosis or the lymphatic system (Serhan et al., 2010).

Severe traumatic injury accompanied by infection or additional tissue damage can lead to a persistent state of inflammatory dysregulation characterized by an overactivation of the innate immune response (primarily neutrophils) followed by a strong anti-inflammatory response that causes suppression of adaptive immunity resulting in decreased T cell function (Valparaiso et al., 2015). Neutrophils release reactive oxygen species (ROS) and proteases to fight pathogens and remove damaged tissue. Even a properly functioning inflammatory response causes some damage to tissue of the host organism (Medzhitov, 2008). When inflammation does not resolve normally, the tissue damage caused by the neutrophil response is injurious and can result in a positive feedback loop that exacerbates the inflammatory response. Lymphocytes are an important component of the adaptive immune response (Barrett et al., 2009) and are crucial for the host response to infection. Reduced lymphocyte levels impair the ability of the host to respond to infection that inevitably accompanies serious traumatic injury. The schematic shown in Figure 4.7 illustrates how tissue injury coupled with physiological and imuunologic disturbances interact to contribute to post-injury morbidity and mortality (Valparaiso et al., 2015).

Disorders that stem from dysregulated inflammation include acute respiratory distress syndrome (ARDS), sepsis, and multiple organ dysfunction syndrome (MODS). These disorders are commonly seen in patients in ICUs. In particular, most ICU patients have some degree of organ dysfunction and as many as 50% have MODS. Mortality from MODS varies depending on the number of organ systems affected, with mortality associated with three or more organ system failures ranging from 20-100% (*Irwin and Rippe's Intensive Care Medicine* 2011). MODS is the most common reason for long stays in the ICU. Given the serious risks associated with inflammation-related disorders resulting from traumatic injuries, it is crucial that the patients most at risk are identified early so interventions and treatments can be appropriately prioritized. The cellular and molecular events that occur during inflammation are similar whether injury occurs through blunt, penetrating, or burn initiating mechanisms; therefore, it is possible to find biomarkers useful for identifying patients at risk of developing disorders of dysregulated inflammation.

A high-level schematic of the body's response to traumatic injury is shown in Figure 4.8 (Lord et al., 2014). Signals produced by stressed, damaged, or malfunctioning tissues act as endogenous inducers of inflammation (Medzhitov, 2008, Kotas and Medzhitov, 2015). The host senses pathogens by both a direct mechanism, where host proteins bind microbial products, and an indirect mechanism, using host molecules that detect products of host

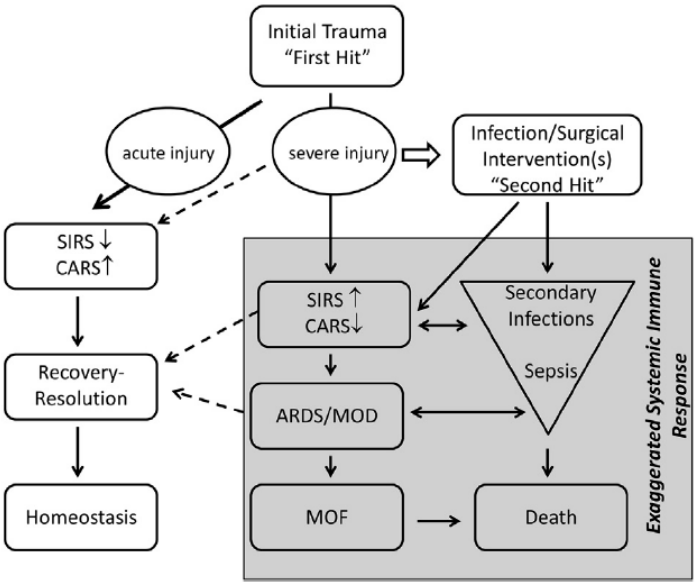

Figure 4.7: Interactions of tissue injury with physiological and immunological disturbances that lead to post-injury morbidity and mortality (Valparaiso et al., 2015).

cell necrosis (Nathan and Ding, 2010). The host uses necrosis of its own cells as one of the immune system's earliest and best-amplified signals to report the dissemination of a possible infection. Damage-associated molecular patterns (DAMPs) are released by injured and necrotic cells in damaged tissue and secreted by neutrophils that have been recruited to the site of injury. DAMPs are potent activators of several types of immune cell, including immune cells that are involved in the complement response. Activation of these cell types triggers the release of numerous inflammatory mediators like cytokines and interleukins. Peptides and DNA released from the mitochondria of damaged cells elicit a particularly potent response, most likely due to the mitochondria of eukaryotes having evolved from an aerobic bacterium living within an archaeal host cell (see the endosymbiotic theory Margulis and Bermudes, 1985). Infection of some degree nearly always accompanies traumatic injury. Damage to the skin or gastrointestinal tract can lead to exposure to exogenous or endogenous pathogens which causes further stress to the patient. Analogous to the DAMPs released or secreted by endogenous cells, infection results in exposure to a number of non-self pathogen-associated molecular patterns (PAMPs) that also activate the immune system (Lord et al., 2014).

4.3.2 NLR Studies

The physiological inflammatory and immune response to various stressful events, including traumatic injury, is characterized by changes in the levels of certain circulating leukocytes (white blood cells) (de Jager et al., 2010). Neutrophil counts typically increase and lymphocyte counts decrease. The neutrophil to lymphocyte ratio (NLR), has been recognized as a biomarker of a patient's level of inflammation and stress (Zahorec, 2001), and an elevated NLR identifies patients that have less physiological reserve to survive the inflammatory insult resulting from a traumatic injury (Salciccioli et al., 2015). The NLR has demonstrated

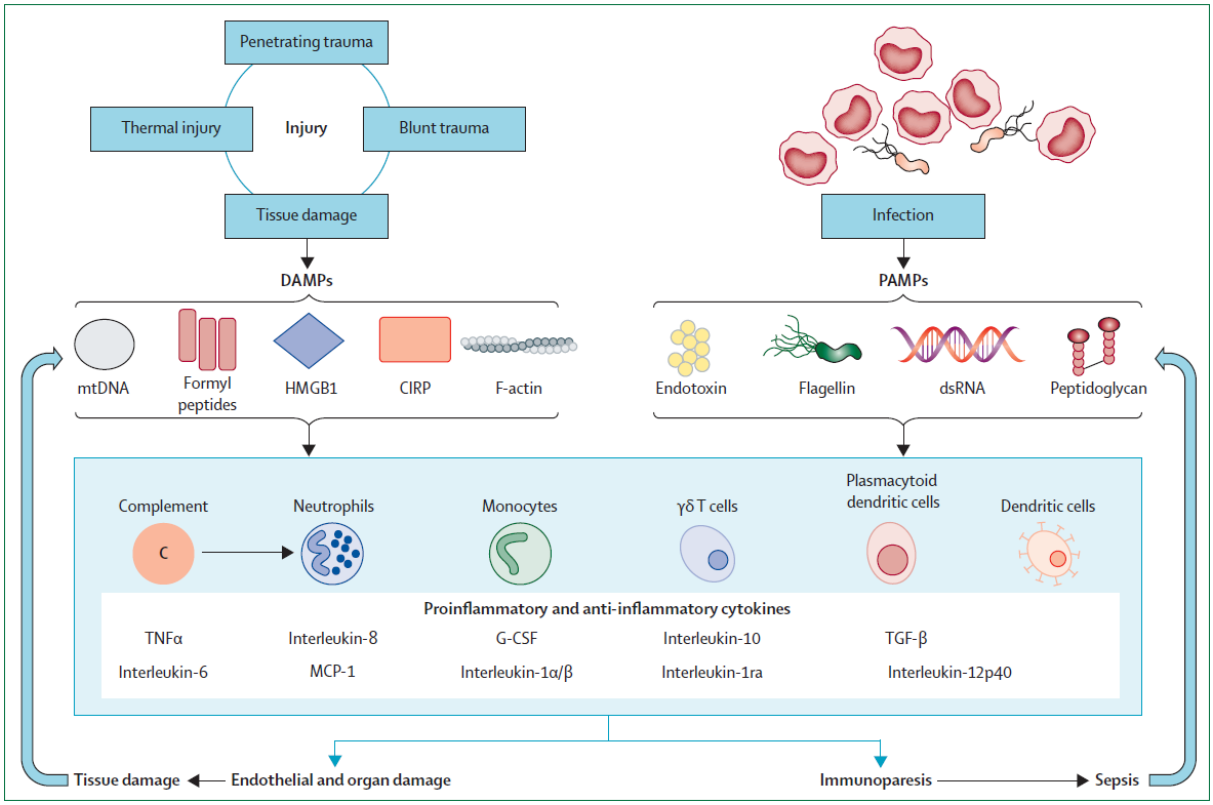

Figure 4.8: Activation of the inflammatory response in response to trauma, tissue damage, and infection (Lord et al., 2014).

prognostic value with trauma patients (Akilli et al., 2014, Dilektasli et al., 2016, Salciccioli et al., 2015), but has also been useful clinically with patients experiencing different types of cancer (Absenger et al., 2013, Rimando et al., 2016, Salman et al., 2016), sepsis (Riché et al., 2015, Salciccioli et al., 2015, Liu et al., 2016), radiation poisoning (Hérodin et al., 2012, Blakely et al., 2014, Ossetrova et al., 2014, Valente et al., 2015), mushroom poisoning (Koylu et al., 2014), and suicide risk in patients with bipolar disorder (Ivković et al., 2016). The NLR is easily obtained using standard clinical measures, and is a fast and efficient means for identifying patients at high risk of potentially deadly complications. The prognostic value of the NLR is a consequence of the centrality and function of these cell types in the inflammatory response.

The NLR has been used as an indicator for a large number of disease groups. Unfortunately, no manuscripts could be found associating NLR with mortality due solely to burns or radiation exposure, the diseases most relevant for use with HENRE. Although, the NLR has been reported as a biomarker of radiation exposure (*The medical aspects of radiation incidents* 2013), detailed information on the derivation of cuttoff values was not provided. Three manuscripts were found that discuss the prognostic value of the NLR in critically ill (Akilli et al., 2014, Salciccioli et al., 2015) or trauma patients (Dilektasli et al., 2016). There are no patients with burn or radiation injuries in these studies; however, the generality of the inflammatory response makes the reasonable assumption that the levels of the NLR associated with mortality will be relevant for different disease groups. This claim is supported

by recent work that found very high correlations among the human transcriptional responses of inflammation-related genes in response to trauma, burns, and endotoxemia (Seok et al., 2013).

The study by Akilli et al., 2014 was a prospective, observational cohort study that followed 373 critically ill patients that were admitted to the emergency department at a single medical center between January 1, 2013 and August 10, 2013. All patients in the study required treatment administered in the ICU. The median age of the patients was 74, and 54.4% were male. The primary endpoints were in-hospital mortality and 6-month mortality. Figure 4.9 shows the receiver operating characteristic (ROC) curve used to find the optimal NLR cutoff for distinguishing between patients that survived and patients that died. ROC analysis is a common technique used to evaluate the predictive power of a biomarker by plotting the true positive rate against the false positive rate, where the biomarker is considered to have significant power if area under the curve (AUC) is much larger than 0.5 (with a maximum of 1). In this case, the optimal NLR cutoff was found by Youden's method (Youden, 1950) to be 11.9. The AUC of the ROC curve is relatively modest at 0.61, indicating that the NLR only weakly discriminates between surviving and non-surviving patients in this study. Kaplan-Meier curves of patients grouped by NLR quartile are shown in Figure 4.10. Survival decreases with increasing NLR quartile.

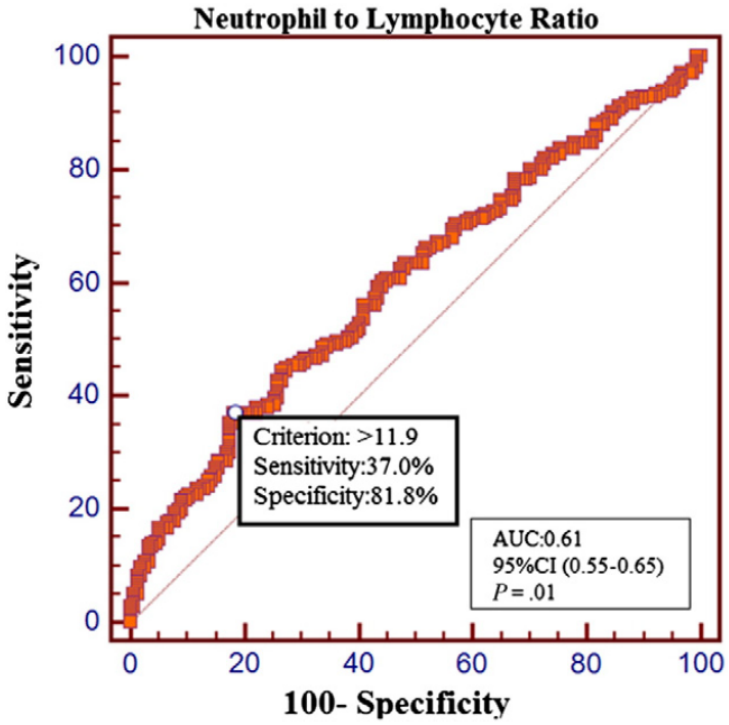

Figure 4.9: Receiver operating characteristic curve of NLR to predict mortality (Akilli et al., 2014).

Salciccioli et al., 2015 also performed an observational cohort study on ICU patients. The study used data collected from the Multiparameter Intelligent Monitoring in Intensive Care (MIMIC II) clinical database Saeed et al., 2011. There were a total of 5,056 patients

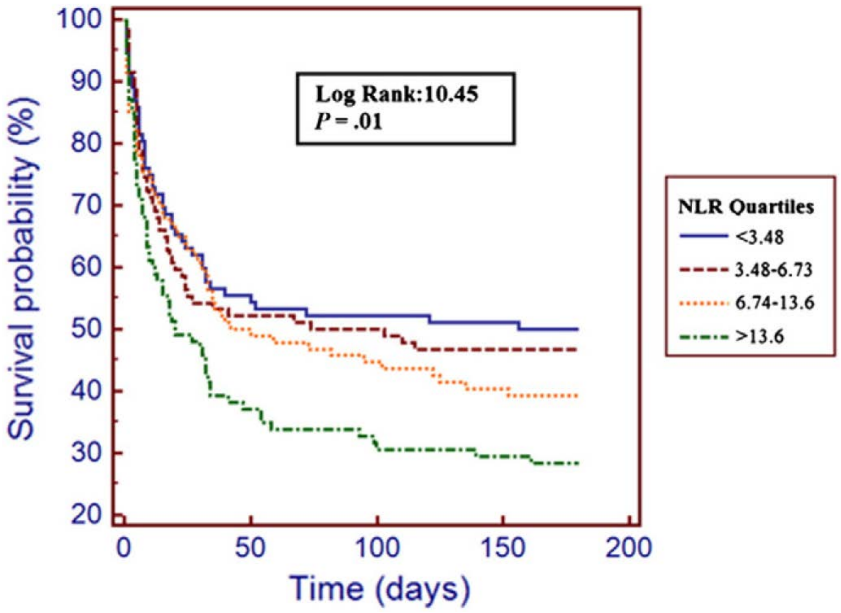

Figure 4.10: Kaplan-Meier survival curves for NLR quartiles determined in Akilli et al., 2014.

that were over 17 years old, had complete neutrophil and lymphocyte data at admission, and had full sets of covariates. The median age was 65 (interquartile range of 51-78), and 53% of the patients were male. The primary endpoint of the study was 28-day mortality, secondary endpoints were in-hospital mortality and 1-year mortality. Subjects were grouped by NLR quartile, with cutpoints at 4.99, 8.90, and 16.21. There was a statistically significant relationship between increasing quartile of NLR quartile and 28-day mortality in an unadjusted analysis over time. The relationship remained significant after adjusting with covariates. All secondary outcomes showed similar trends in mortality. The relationship between NLR quartile and mortality is also illustrated by Figure 4.11 using the data from the study by Salciccioli et al., 2015.

The Dilektasli et al., 2016 study is a retrospective cohort study consisting of 1,007 trauma patients 16 years or older admitted to the surgical intensive care unit of the LAC + USC Medical Center between January 2013 and January 2014. The median age was 49 and 74% were male. The performance of the classifiers from the Dilektasli et al., 2016 manuscript can be seen in Figure 4.12, which shows the ROC curves obtained for NLR values measured on hospital days 2 and 5. Optimal cutoff values distinguishing patients that died and survived in the first 10 days of hospitalization were determined using the Youden index and found to be 8.19 for hospital day 2 and 7.92 for hospital day 5. A higher NLR, measured at 2 or 5 days, was significantly associated with higher in-hospital mortality and with reduced overall survival. Kaplan Meier curves of the overall survival where patients were stratified using the cutoff values determined by the ROC analysis are shown in Figure 4.13.

The median ages of the study populations in the Akilli et al., 2014 and Salciccioli et al., 2015 studies are high. Many of the patients in these study populations are likely suffering from complicated geriatric syndromes or complications related to chronic diseases. The sample size of the Akilli et al., 2014 study is also relatively small. The population studied

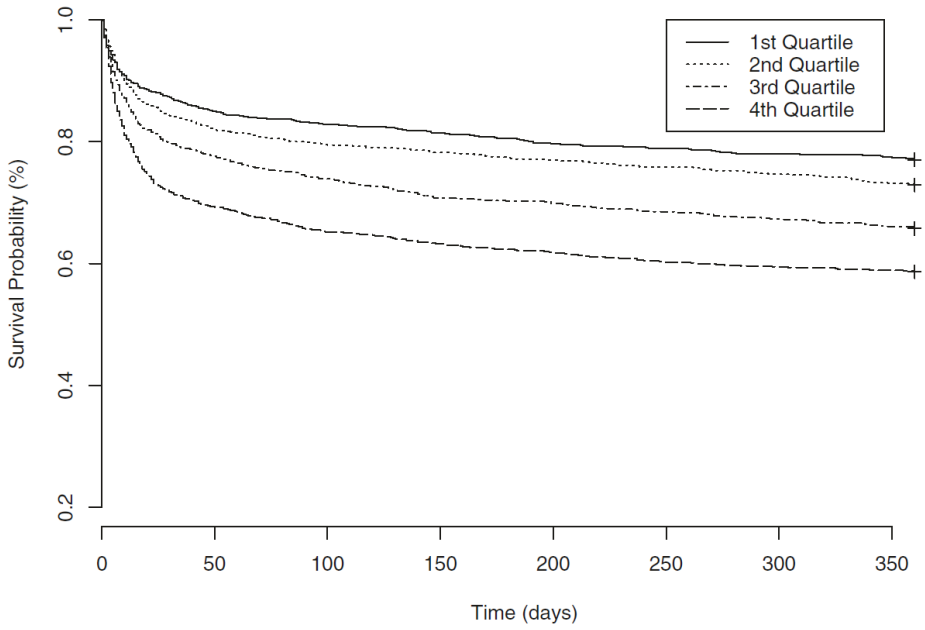

Figure 4.11: Kaplan-Meier survival curves for 1-year mortality based on NLR quartiles determined in Salciccioli et al., 2015. Quartile cutpoints were NLR values of 4.99, 8.90, and 16.21. Patients in the fourth NLR quartile (NLR>16.21 had the lowest survival probability at one year.

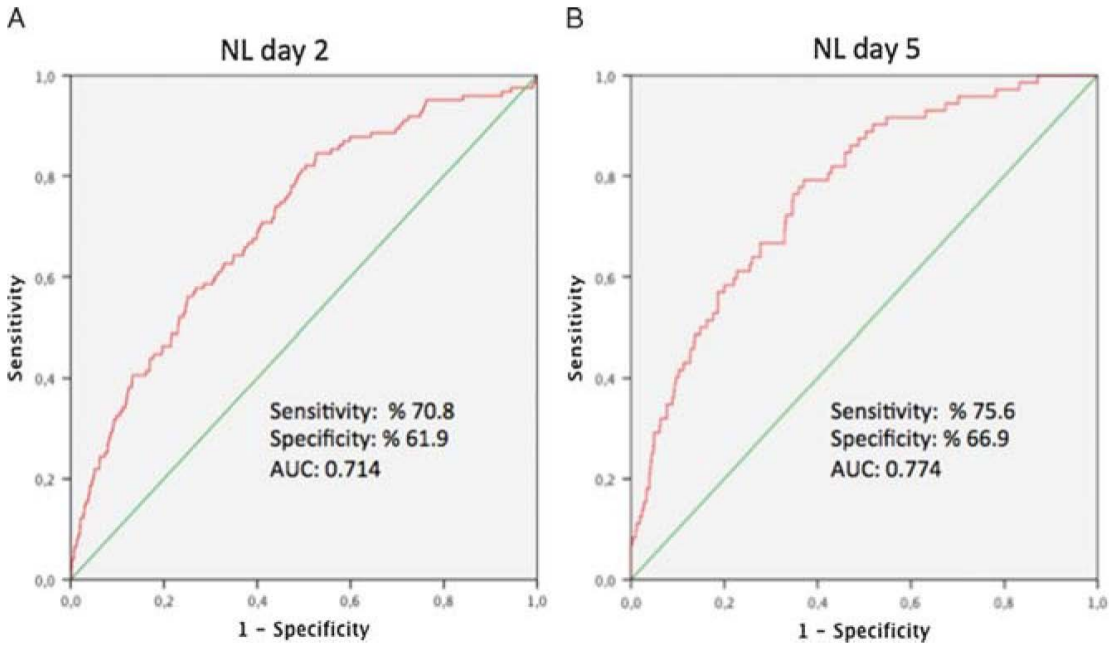

Figure 4.12: ROC curves for (**A**) the NLR on hospital day 2 and (**B**) hospital day 5 (Dilektasli et al., 2016).

in Dilektasli et al., 2016 consists primarily of patients admitted to the ICU for blunt or penetrating injuries. The median age of the study population is considerably lower than

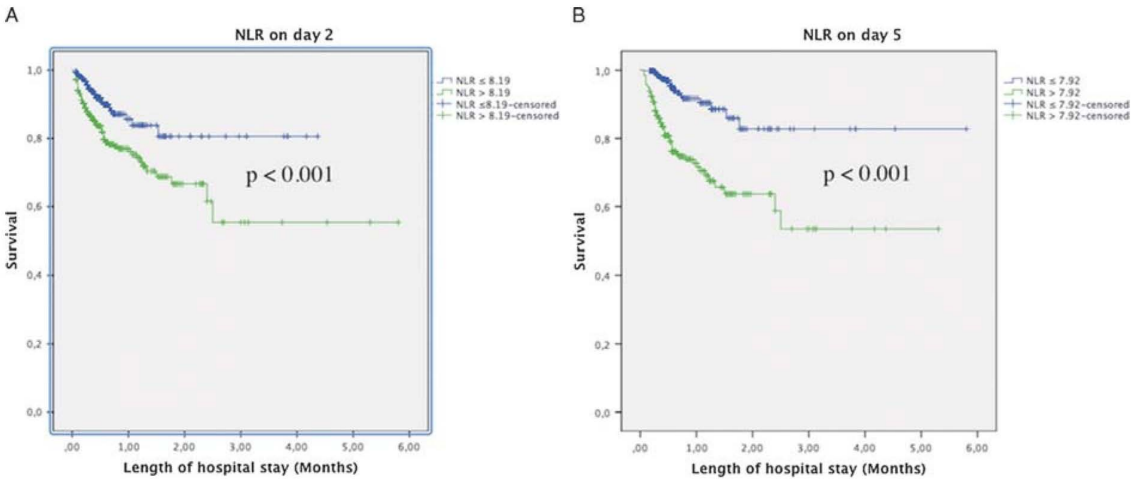

Figure 4.13: Kaplan Meier survival curves for (**A**) the day 2 cutoff of 8.19 and (**B**) the day 2 cutoff of 7.92 (Dilektasli et al., 2016).

those of the Akilli et al., 2014 and Salciccioli et al., 2015 populations.

HENRE contains models that describe the dynamics of lymphocyte and granulocyte populations in response to burn or radiation injury (Wentz et al., 2014a, Wentz et al., 2015). Currently, these models represent part of the complex biology associated with inflammation; for example, they do not simulate the processes associated with dysregulated inflammation that would be expected to be seen on the pathway to ARDS, sepsis, and MODS. A quantitative model relating the NLR to mortality would not be useful at this time given the limited biological domain of the existing models and state of the available data. However, this section demonstrates the centrality of the inflammatory process in the combined-injury scenario and suggests directions for further development of the capabilities of HENRE.

5 Results

The gastrointestinal subsyndrome of ARS is expected to play a large role in 30-day mortality, and our model allows us to quantify the added risk of mortality from burns for ARS casualties. Figure 5.1 presents predictions of 30-day mortality from various radiation and burn combined injuries (CIs) calculated from the SIMM. These simulations are presented as radiation dose response curves at fixed burn insults. With no burn (0% TBSA), the model predicts an LD50/30 (the lethal dose for 50% of the population by day 30) of approximately 12.5 Gy (MLT). This is a very large radiation dose, but it lies in an expected range when compared to other lethal doses. For example, the human LD50/60 assuming no treatment is estimated to be 4.34 Gy (MLT) (Stricklin, 2015b), and the LD50/48hr (the lethal dose for 50% of the population by 48 hours) assuming no treatment has been estimated to be 31 Gy (MLT) (Millage and Crary, 2016).

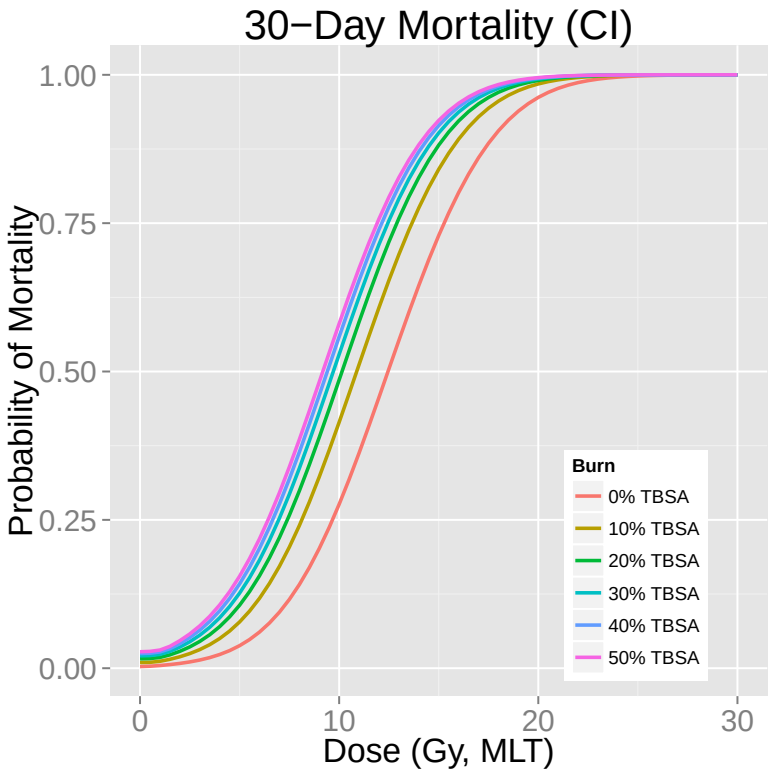

Figure 5.1: Probability of 30-day mortality predicted using the SIMM.

These results suggest that the contribution of burn (measured by % TBSA) to GI-ARS-related mortality is relatively minor. This can be attributed to the fact that the SIMM only accounts for death from bacterial translocation through the breakdown of the small intestine epithelial lining. Because the small intestine model was initially developed with the intention of modeling ARS, the SIMM does not account for mortality from risks such as wound infections associated with burns. Although bacterial translocation is a primary

contributing factor to death for GI-ARS, infection through burn wounds is particularly lethal when burns exceed 40% TBSA (Gang et al., 1999; Taneja et al., 2004). For this reason, we assume the model is appropriate for low to medium burn sizes.

Results from the PAMM are provided in Figure 5.2. The LA50/60 (the percentage of the body surface area burned in which 50% mortality results by day 60) from this model is approximately 37%, which is slightly higher than the LA50/60 of 45% predicted by our 60-day mortality model assuming no treatment (Stricklin, 2013b). Although we would expect to see a higher LA50/60 here, it is encouraging to see that these numbers are fairly similar. We intend to revisit this inconsistency in future studies.

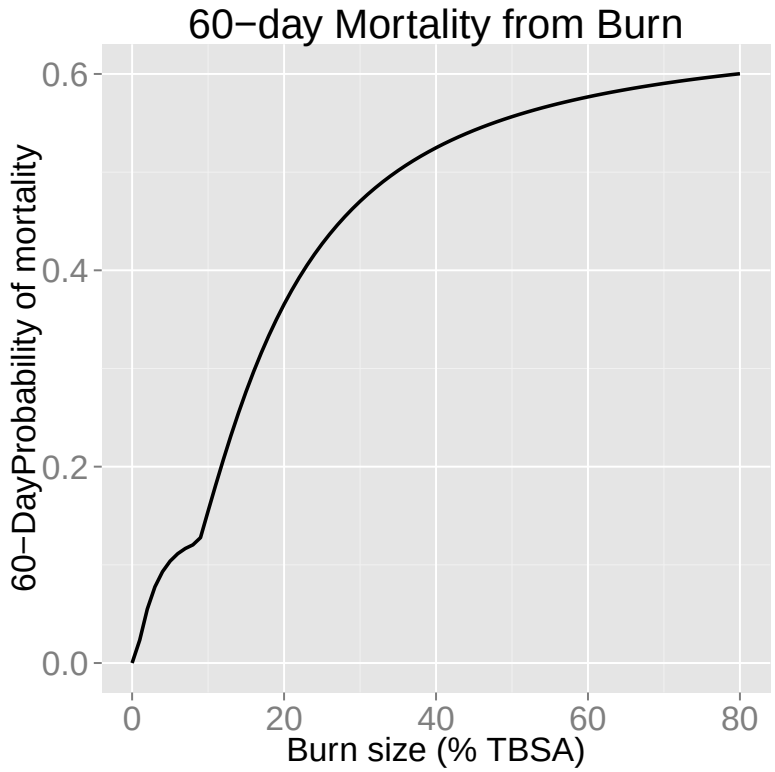

Figure 5.2: Probability of 60-day mortality predicted from platelet reduction.

Together, the SIMM and PAMM provide new capabilities for the 30 and 60-day mortality models currently in HENRE. The SIMM is a first step in developing combined injury capabilities of the 30-day mortality model, and the PAMM is a first step in predicting 60-day mortality with treatment.

6 Discussion

The purpose of this study was to develop models that predict the probability of death of an individual through the use of predictive biomarkers. We used relevant hospital patient data to correlate biomarker levels with the probability of 30 and 60-day mortality. Models that represent cell kinetics were used to predict biomarker levels, which in turn were used to predict mortality.

The SIMM and PAMM continue to build capabilities in HENRE to predict mortality due to combined injury. These models consider the difference in health outcomes for individuals receiving standard care, and represent significant steps in capturing critical physiological processes and systems affected by radiation and burn. The majority of the models previously developed for this effort operate under the assumption that no treatment is available. Currently, the 60-day mortality model in HENRE is capable of taking treatment into account for the radiation environment.

As with all models, there are limitations to the SIMM and PAMM, most notably, with respect to the domain of applicability suggested by the underlying data. The SIMM, for example, predicts the probability of mortality due to GI-ARS for combined radiation and burn injury. However, we recognize that the model development was driven primarily by studies on radiation effects. Burn complicates the physiological response considerably in ways that are not currently well represented in the literature, particularly at lower radiation levels. Consequently, we believe that the domain of applicability for the SIMM is limited to radiation and burn environments as depicted in Figure 6.1 A. That is, the reliability of the model predictions is considered to be higher for environments in which the radiation exposure is relatively high, and the % TBSA is relatively low.

For the PAMM, we noted earlier that the maximum probability of mortality is 66%, even at 100% platelet loss. As with the SIMM, the PAMM is not considered reliable for significant burns (e.g., in excess of 60% TBSA) because it does not adequately capture the physiological response and elevated risk for burns of this magnitude. This, of course, is a limitation of any model that explains the response phenomena for an insult that, in reality, elicits a suite of physiological responses with increasing damage. The domain of applicability for the PAMM is represented by Figure 6.1 B.

Lastly, the research that we conducted on the NLR underscored the need for discussion regarding the utility of building out response-specific models that are not fully integrated with other mechanistic models in HENRE. Although the research on NLR is promising, the benefit of adding an NLR model based on currently available data was considered to be negligible. However, implicit in the discussion of inflammatory response physiology in Section 4.3, is the need to consider "next generation" capabilities for HENRE, namely, the full integration of response-specific models within a framework that includes inflammation at its core. Ultimately, the fidelity of HENRE's predictions on injury severity and the time course of disease will depend on the ability of the model to integrate exposure and effect through time for alternative treatment scenarios. The NLR discussion provides an excellent basis for "next gen" discussions that will shape the future development of HENRE capabilities.

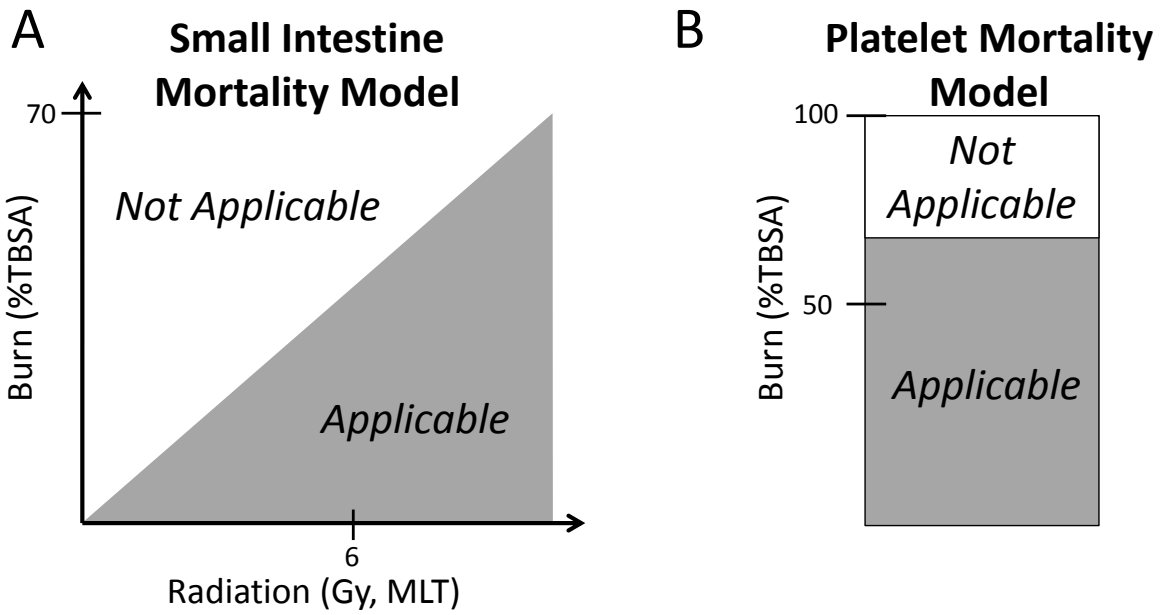

Figure 6.1: Domain of applicability for the small intestine and platelet mortality models.

7 Future Work

We continuously aim to improve each of the components of HENRE. The models in this study were developed to expand the domain of applicability of the 30 and 60-day mortality models in HENRE by accounting for treatment of individuals exposed to IND environments. We recognize that there are limitations for these models, and we aim to address these in future studies. This can be accomplished by collecting more data to train and validate our models, as well as performing sensitivity and uncertainty analysis to test the reliability of the models.

In order to continue to improve the capability of the mortality models in HENRE, we also aim to expand the context with which our mortality models are defined. For instance, the mortality models only account for demographics (age and gender) in the context of 60-day radiation-induced mortality. In the future, we would like to account for demographics in the 30-day and 48-hour models. We would also like to account for demographic modifications in the context of combined injury. In addition, we would like to assess the use of the NLR to predict mortality with the granulocyte and lymphocyte cell kinetic models built into HENRE.

References

Absenger, G et al. (2013). "Preoperative neutrophil-to-lymphocyte ratio predicts clinical outcome in patients with stage II and III colon cancer." In: *Anticancer Res* 33.10, pp. 4591–4594.

Akca, S et al. (2002). "Time course of platelet counts in critically ill patients". In: *Critical care medicine* 30.4, pp. 753–756.

Akilli, NB et al. (2014). "Prognostic importance of neutrophil-lymphocyte ratio in critically ill patients: short- and long-term outcomes." In: *Am J Emerg Med* 32.12, pp. 1476–1480.

Ashley, NT, ZM Weil, and RJ Nelson (2012). "Inflammation: Mechanisms, costs, and natural variation". In: *Annu. Rev. Ecol. Evol. Syst.* 43.1, pp. 385–406.

Baker, DG and FA Valeriote (1968). "The effect of x-irradiation and thermal burn on the intestinal mucosa". In: *Canadian journal of physiology and pharmacology* 46.3, pp. 533–536.

Barrett, KE et al. (2009). *Ganong's review of medical physiology (enhanced EB)*. McGraw-Hill Education.

Bellman, J (2016). *Small intestine villus count decline as a prognostic indicator of 30-day mortality*. Tech. rep. ARA/HS-TN-16-014. Applied Research Associates, Inc.

Bellman, J and D Stricklin (2016). *A mathematical model of the human small intestine following acute radiation and burn exposures*. Tech. rep. DTRA-TR-16-059.

Blakely, WF et al. (2014). "Further biodosimetry investigations using murine partial-body irradiation model." In: *Radiat Prot Dosimetry* 159.1-4, pp. 46–51.

Bond, VP, TM Fliedner, and JO Archambeau (1965). *Mammalian radiation lethality: A disturbance in cellular kinetics*. Academic Press, New York, pp. 78–83.

Carter, SR et al. (2016). "Neutrophil accumulation in the small intestine contributes to local tissue destruction following combined radiation and burn injury:" in: *Journal of Burn Care & Research* 37.2, pp. 97–105.

Crary, D (2016). *Platelet count decline as a prognostic indicator of lethality in ICU and burn patients*. Tech. rep. DTRA-TR-16-012.

Crenn, P et al. (2000). "Postabsorptive plasma citrulline concentration is a marker of absorptive enterocyte mass and intestinal failure in humans". In: *Gastroenterology* 119.6, pp. 1496–1505.

Crenn, P et al. (2014). "Plasma l-citrulline concentrations and its relationship with inflammation at the onset of septic shock: A pilot study". In: *Journal of Critical Care* 29.2, 315.e1–315.e6.

Curis, E et al. (2005). "Almost all about citrulline in mammals". In: *Amino Acids* 29.3, pp. 177–205.

de Jager, CPC et al. (2010). "Lymphocytopenia and neutrophil-lymphocyte count ratio predict bacteremia better than conventional infection markers in an emergency care unit." In: *Crit Care* 14.5, R192.

Dilektasli, E et al. (2016). "The prognostic value of neutrophil to lymphocyte ratio on mortality in critically Ill trauma patients." In: *J Trauma Acute Care Surg.*

Gang, R et al. (1999). "Pseudomonas aeruginosa septicaemia in burns". In: *Burns* 25.7, pp. 611–616.

Guo, F et al. (2012). "Association of platelet counts decline and mortality in severely burnt patients". In: *Journal of Critical Care* 27.5, 529.e1–529.e7.

Guoyao, WU and SM Morris (1998). "Arginine metabolism: nitric oxide and beyond". In: *Biochemical Journal* 336.1, pp. 1–17.

Hempelmann, LH, H Lisco, and JG Hoffman (1952). "The acute radiation syndrome: a study of nine cases and a review of the problem". In: *Annals of Internal Medicine* 36.2:1, pp. 279–510.

Hérodin, F et al. (2012). "Assessment of total- and partial-body irradiation in a baboon model: preliminary results of a kinetic study including clinical, physical, and biological parameters." In: *Health Phys* 103.2, pp. 143–149.

Howland, JW et al. (1961). *Diagnosis and treatment of acute radiation injury: proceedings of a scientific meeting jointly sponsored by the IAEA and the WHO, Geneva, 17-21 Oct 1960*. Columbia University Press, New York, pp. 11–26.

Irwin and Rippe's Intensive Care Medicine (2011). Lippincott Williams & Wilki.

Ivković, M et al. (2016). "Neutrophil-to-lymphocyte ratio predicting suicide risk in euthymic patients with bipolar disorder: Moderatory effect of family history." In: *Compr Psychiatry* 66, pp. 87–95.

Jianfeng, G et al. (2005). "Serum citrulline is a simple quantitative marker for small intestinal enterocytes mass and absorption function in short bowel patients". In: *Journal of Surgical Research* 127.2, pp. 177–182.

Kiang, JG et al. (2014). "Ghrelin therapy improves survival after whole-body ionizing irradiation or combined with burn or wound: amelioration of leukocytopenia, thrombocytopenia, splenomegaly, and bone marrow injury". In: *Oxidative Medicine and Cellular Longevity* 2014, pp. 1–12.

Kotas, ME and R Medzhitov (2015). "Homeostasis, inflammation, and disease susceptibility." In: *Cell* 160 (5), pp. 816–827.

Koylu, R et al. (2014). "Influence of neutrophil/lymphocyte ratio on prognosis in mushroom poisoning". In: *Acta Med Mediterr* 30, pp. 849–864.

Liu, X et al. (2016). "Prognostic significance of neutrophil-to-lymphocyte ratio in patients with sepsis: A prospective observational study." In: *Mediators Inflamm* 2016.

Lord, JM et al. (2014). "The systemic immune response to trauma: an overview of pathophysiology and treatment." In: *Lancet (London, England)* 384 (9952), pp. 1455–1465.

Luo, M et al. (2007). "Are plasma citrulline and glutamine biomarkers of intestinal absorptive function in patients with short bowel syndrome?" In: *Journal of Parenteral and Enteral Nutrition* 31.1, pp. 1–7.

Maciàă I Garau, M, A Lucas Calduch, and EC López (2011). "Radiobiology of the acute radiation syndrome." In: *Reports of practical oncology and radiotherapy : journal of Greatpoland Cancer Center in Poznan and Polish Society of Radiation Oncology* 16 (4), pp. 123–130.

Marck, RE et al. (2013). "Time course of thrombocytes in burn patients and its predictive value for outcome". In: *Burns* 39.4, pp. 714–722.

Margulis, L and D Bermudes (1985). "Symbiosis as a mechanism of evolution: status of cell symbiosis theory." In: *Symbiosis (Philadelphia, Pa.)* 1. Grant numbers: NGR 004-025, pp. 101–124.

Medzhitov, R (2008). "Origin and physiological roles of inflammation." In: *Nature* 454 (7203), pp. 428–435.

Mettler, FA (2001). *Medical management of radiation accidents*. Ed. by IA Gusev, AK Guskova, and FA Mettler. 2nd. CRC Press, Boca Raton, pp. 211–222.

Millage, K and D Crary (2016). *Probability of mortality within 48 hours from radiation alone*. Tech. rep. DTRA-TR-16-011. Applied Research Associates, Inc.

Moreau, D et al. (2007). "Platelet count decline: an early prognostic marker in critically ill patients with prolonged ICU stays". In: *CHEST Journal* 131.6, pp. 1735–1741.

Nathan, C and A Ding (2010). "Nonresolving inflammation." In: *Cell* 140 (6), pp. 871–882.

Oldson, D, J Wentz, and D Stricklin (2015). *HENRE 2.0 technical reference manual.* Tech. rep. DTRA-TR-15-070.

Ossetrova, NI et al. (2014). "Early-response biomarkers for assessment of radiation exposure in a mouse total-body irradiation model." In: *Health Phys* 106.6, pp. 772–786.

Palmer, JL et al. (2011). "Development of a combined radiation and burn injury model". In: *Journal of Burn Care & Research* 32.2, pp. 317–323.

Pappas, PA et al. (2002). "Serum citrulline as a marker of acute cellular rejection for intestinal transplantation". In: *Transplantation proceedings*. Vol. 34. Elsevier, pp. 915–917.

Piton, G et al. (2010). "Plasma citrulline kinetics and prognostic value in critically ill patients". In: *Intensive Care Medicine* 36.4, pp. 702–706.

Piton, G et al. (2011). "Acute intestinal failure in critically ill patients: is plasma citrulline the right marker?" In: *Intensive Care Medicine* 37.6, pp. 911–917.

Piton, G et al. (2013). "Enterocyte damage in critically ill patients is associated with shock condition and 28-day mortality". In: *Critical Care Medicine* 41.9, pp. 2169–2176.

Rhoads, JM et al. (2005). "Serum citrulline levels correlate with enteral tolerance and bowel length in infants with short bowel syndrome". In: *The Journal of Pediatrics* 146.4, pp. 542–547.

Riché, F et al. (2015). "Reversal of neutrophil-to-lymphocyte count ratio in early versus late death from septic shock." In: *Crit Care* 19.

Rimando, J et al. (2016). "The pretreatment neutrophil/lymphocyte ratio is associated with all-cause mortality in black and white patients with non-metastatic breast cancer." In: *Front Oncol* 6.

Saeed, M et al. (2011). "Multiparameter Intelligent Monitoring in Intensive Care II: A public-access intensive care unit database". In: *Critical Care Medicine* 39.5, pp. 952–960.

Salciccioli, JD et al. (2015). "The association between the neutrophil-to-lymphocyte ratio and mortality in critical illness: an observational cohort study." In: *Crit Care* 19.

Salman, T et al. (2016). "Prognostic value of the pretreatment neutrophil-to-lymphocyte ratio and platelet-to-lymphocyte ratio for patients with neuroendocrine tumors: An Izmir Oncology Group study." In: *Chemotherapy* 61.6, pp. 281–286.

Seok, J et al. (2013). "Genomic responses in mouse models poorly mimic human inflammatory diseases." In: *Proceedings of the National Academy of Sciences of the United States of America* 110 (9), pp. 3507–3512.

Serhan, CN, PA Ward, and DW Gilroy (2010). *Fundamentals of inflammation*. Cambridge University Press.

Stavem, P et al. (1985). "Lethal acute gamma radiation accident at Kjeller, Norway: Report of a case". In: *Acta Radiologica: Oncology* 24.1, pp. 61–63.

Strauss, R et al. (2002). "Thrombocytopenia in patients in the medical intensive care unit: bleeding prevalence, transfusion requirements, and outcome". In: *Critical care medicine* 30.8, pp. 1765–1771.

Stricklin, D. (2013a). *Estimation of radiation permeability parameters for integration into the CSM model*. Tech. rep. ARA/HS-TN-13-012. Applied Research Associates, Inc.

Stricklin, D (2013b). *Estimation of radiation permeability parameters for integration into the CSM model*. Tech. rep. ARA/HS-TN-13-012. Applied Research Associates, Inc.

— (2015a). *Selection of a dose response relationship for radiation lethality with treatment for implementation in HENRE*. Tech. rep. DTRA-TR-15-007. Applied Research Associates, Inc.

Stricklin, D. (2015b). *Selection of a dose response relationship for Radiation lethality with treatment for implementation in HENRE*. Tech. rep. DTRA-TR-15-007. Applied Research Associates, Inc.

Stricklin, D (2016). *Selection of demographic modification factors for radiation lethality for implementation in HENRE: Age and Gender*. Tech. rep. ARA/HS-TN-16-001. Applied Research Associates, Inc.

Su, L et al. (2015). "Dynamic changes in amino acid concentration profiles in patients with sepsis". In: *PloS one* 10.4, e0121933.

Taneja, N et al. (2004). "A prospective study of hospital-acquired infections in burn patients at a tertiary care referral centre in North India". In: *Burns* 30.7, pp. 665–669.

The medical aspects of radiation incidents (2013). Radiation Emergency Assistance Center/Training Site REACT/TS.

Valente, M et al. (2015). "Revisiting biomarkers of total-body and partial-body exposure in a baboon model of irradiation". In: *PLoS One* 10.7, e0132194.

Valparaiso, A et al. (2015). "Modeling acute traumatic injury". In: *Journal of Surgical Research* 194.1, pp. 220–232.

Vanderschueren, S et al. (2000). "Thrombocytopenia and prognosis in intensive care". In: *Critical care medicine* 28.6, pp. 1871–1876.

Wentz, J, D Oldson, and D Stricklin (2014a). *Mathematical models of human hematopoiesis following acute radiation exposure*. Tech. rep. DTRA01-03-D-0014. Applied Research Associates, Inc.

— (2014b). "Modeling the thrombopoietic effects of burn". In: *Letters in Biomathematics* 1.1, pp. 111–126.

— (2015). *Models of hematopoietic dynamics following burn for use in combined injury simulations*. Tech. rep. HDTRA1-14-D-003; 0005. Nuclear Survivability and Forensics Integrated Program Team.

Wijnands, K et al. (2015). "Arginine and citrulline and the immune response in sepsis". In: *Nutrients* 7.3, pp. 1426–1463.

Youden, W (1950). "Index for rating diagnostic tests". In: *Cancer* 3.1, pp. 32–35.

Zahorec, R (2001). "Ratio of neutrophil to lymphocyte counts–rapid and simple parameter of systemic inflammation and stress in critically ill." In: *Bratisl Lek Listy* 102.1, pp. 5–14.

8 Abbreviations, Acronyms and Symbols

ARA	Applied Research Associates, Inc.
ARDS	Acute respiratory distress syndrome
ARS	Acute radiation syndrome
AUC	Area under the curve
CI	Combined injury
d	Days
DAMP	Damage-associated molecular pattern
DTRA	Defense Threat Reduction Agency
GI-ARS	Gastrointestinal acute radiation syndrome
Gy	Gray
H-ARS	Hematopoietic acute radiation syndrome
HENRE	Health Effects from Nuclear and Radiological Environments
ICU	Intensive care unit
IND	Improvised nuclear device
MLT	Midline tissue
MIMIC	Multiparameter Intelligent Monitoring in Intensive Care
MODS	Multiple organ dysfunction syndrome
NLR	Neutrophil:lymphocyte ratio
PAMP	Pathogen-associated molecular pattern
PAMM	Platelet Attenuation Mortality Model
ROC	Receiver operating characteristic
ROS	Reactive oxygen species
SBS	Short bowel syndrome
SIMM	Small Intestine Mortality Model
WMD	Weapons of mass destruction
% TBSA	Percent of total body surface area

A Small Intestine Model Update

There is no time-dependent human data of small intestine epithelial cells following burn, which makes it difficult to choose values for the parameters of the small intestine model related to burn response, a_0, b_0, k, a_1, b_1, and Δ_b. In Bellman and Stricklin, 2016, these parameters were chosen by fitting the model to murine data that had been rescaled to more realistic timing and amplitude expected for human response. Unfortunately, the parameter set chosen forced a biologically unrealistic decrease in villus cells. A matrix of combined injury response of villus cells with the original parameter set is presented in Figure A.1.

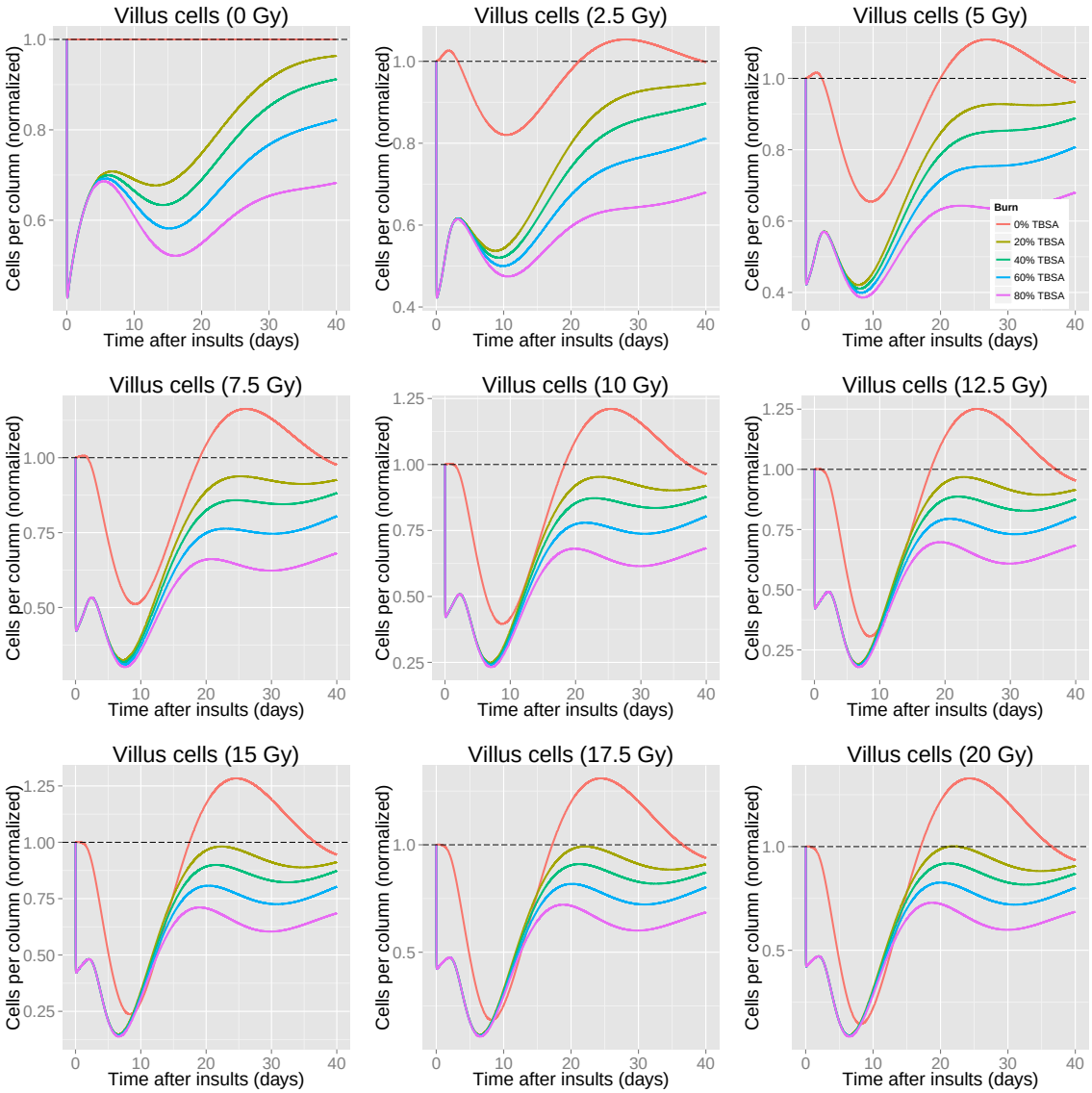

Figure A.1: Small intestine combined injury villus response with previous burn parameters (Table A.1).

We have re-parameterized the burn parameters of the human model under the following conditions:

- We do not scale the amplitude of the murine data as we assume the amplitude of the normalized response to burn is similar between mice and humans. This is supported by the fact that our human and murine models have similar normalized nadirs in response to acute radiation.
- We rescale the timing of proliferation suppression following burn for the human model, Δ_b, based on the relative time difference between human and murine nadirs following acute 5 Gy radiation doses.
- We apply a penalty in our cost function for the time and value of the nadir to ensure that the model does not suffer the same abrupt drop in villus cells following burn.

After performing optimization on the human burn parameters (see details in Bellman and Stricklin, 2016), we compare the updated burn parameters to the original values in Table A.1. An updated matrix of combined injury response is provided in Figure A.2.

Table A.1: Biological descriptions, parameters and variables for burn response in the small intestine mathematical model.

Parameter	Biological Description	Previous Value	Updated Value
a_0	Determines duration of burn effect on villus death	54.919 d^{-1}	0.33 d^{-1}
b_0	Describes maximum effect on villus death	47.986	0.36
a_1	Determines duration of burn effect on proliferation	0.001 d^{-1}	0.0005 d^{-1}
b_1	Describes maximum effect of burn on proliferation	0.767	0.15
k	Activation threshold for burn effect	0.008 %TBSA	18.83 %TBSA
Δ_b	Delay after burn before proliferation suppression	1 d	3.84 d

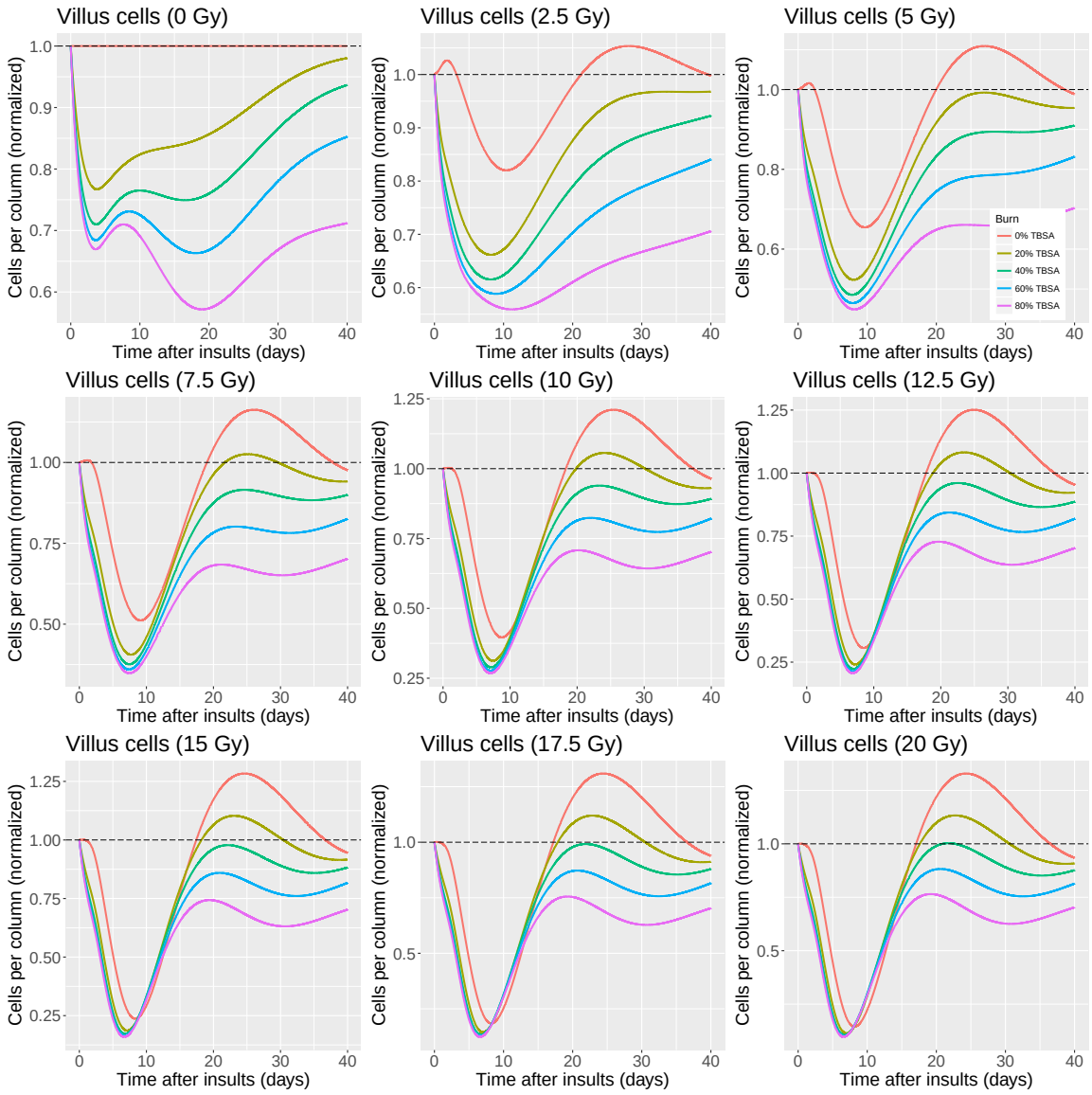

Figure A.2: Small intestine combined injury villus response with updated burn parameters (Table A.1).